# ORCA – Online Research @ Cardiff

# Features Characterizing the Surface State of HV Insulator Glass Model under Desert Pollution

## D. Maadjoudj
Laboratoire de Recherche en Electrotechnique, Ecole Nationale Polytechnique,
El-Harrach, 16200 Algiers, Algeria

## O. Kherif
Advanced High Voltage Engineering Research Centre, School of Engineering, Cardiff University
Cardiff CF24 3AA, U.K.

## A. Mekhaldi and M. Teguar
Laboratoire de Recherche en Electrotechnique, Ecole Nationale Polytechnique,
El-Harrach, 16200 Algiers, Algeria

## ABSTRACT
**This paper deals with the monitoring of the surface state of HV insulator model under discontinuous layer of pollution. Natural desert sand is used to simulate the pollution influence in Algerian Sahara regions. Experimental tests are carried out on a glass plane model of 1512L cap-pin insulator largely used in the said regions. Leakage current LC signal is recorded for different positions and widths of the polluted-band. First, the obtained results are discussed to describe the behaviour of insulator model. For each configuration, time-frequency decomposition is established using Discrete Wavelet Transform (DWT) for information extraction corresponding to the flashover process. Decomposition results indicate that the detail D3 is highly correlated with the measured LC signal. Recurrence Plot (RP) technique and Recurrence Quantification Analysis (RQA) are applied to quantify the temporal patterning in LC signal, giving information on the position and width of the polluted-band on the insulating surface. It was found that RQA indicators increase with the polluted-band width according to the position of this polluted-band. Based on the plan model, the findings demonstrate the capability of RQA indicators for the glass insulator monitoring, providing information on the width and position of the polluted-band on its surface.**

**Index Terms — Desert pollution, industrial insulator, leakage current, non-uniform pollution, signal processing.**

## NOMENCLATURE

| | |
|---|---|
| ENTR | Entropy (Shannon entropy). |
| ESDD | Equivalent salt deposit density. |
| DET | Determinism. |
| DWT | Discrete wavelet technique. |
| LC | Leakage current. |
| NSDD | Non-soluble deposit density. |
| RP | Recurrence plot. |
| RQA | Recurrence quantification analysis. |
| RR | Recurrence rate. |
| STD | Standard deviation. |
| THD | Total harmonic distortion. |

## 1 INTRODUCTION

**INSTALLED** power generation capacity has gradually increased over the years, and the transportation of its large blocks of electrical power over long distances becomes crucial. The configuration of electrical transmission systems varies according to the regions and/or the transport voltage level. Because of certain influencing factors and constraints, it is difficult to choose a common form of insulation with satisfactory performance. For instance, the insulation capacity can be reduced if an insulating chain is exposed to polluted environments and then subjected to high humidity [1]. This initially leads to electric discharges where their severity and rate may increase, generating a complete line-to-ground discharge called ``bypass or flashover'' [2]. This discharge is mostly caused by saline contaminants or insoluble substances on the insulator surface in the presence of moisture [3].

In desert areas, a polluted layer can be developed on the insulator surface by means of gradual accumulations of sand grains during the sandstorm period [4]. Humidification of such a polluted layer causes the passage of an LC through the polluted surface of the insulator [5]. Depending on insulator shape, pollution distribution and wetness degree, the potential distribution is differently affected [6]. In certain cases, the voltage gradient may exceed the critical level to initiate a surface arc, which either extinguishes or evolves to a point leading to the flashover. This later causes several outages within the electric networks [7]. In order to take precautions against possible accidents due to the pollution, a consistent system for monitoring the contamination on insulators surface is powerfully anticipated.

In literature, several investigations have been performed on polluted insulators (e.g., [8], [9]). These include theoretical studies and experiments carried out for better understanding the flashover process and to find efficient tools, monitoring the pollution severity for avoiding the complete flashover. In this light, different methods have been used for monitoring the contamination level. These methods mainly include the leakage current, air pollution measurements, the surface conductance, and optical measurements [10]. Correspondingly, numerous techniques have been developed to predict the contamination level and monitor HV insulators.

Indeed, information extraction, from the leakage current using mathematical tools of signal processing, has been widely used (e.g., [11]—[13]). Li et al. [11] highlighted the mean value, the maximum value and the STD of LC as suitable quantities to study the insulator state under pollution conditions. Fernando et al. [12] studied the dependence of LC pattern on the contaminated surface using a neural network to identify the non-linearity of the LC and its harmonic contents. Moreover, Jiang et al. [13] utilized the phase angle (between LC and applied voltage), the maximum pulse amplitude of LC and the THD as characteristic parameters to assess polluted insulators state. Moula et al. [14] used the wavelet transform to detect the presence of partial arcs on the insulator surface for different configurations of pollution. Using RP and RQA techniques, authors in [15] and [16] carried out a classification of the pollution severity of the insulator surface. Based on FFT, authors in [17]—[21] analysed the LC waveforms for monitoring the degradation of the insulator surface, and the pollution level. Other investigations (e.g., [16], [22]) also showed the strong correlation between the electric phenomena appearing on the insulating surface and the LC signals.

Overall, the majority of the performed studies dealt with cases of a uniform layer covering the entire surface of the insulation. In [4], for instance, authors focused on the effect of the sand quantity in terms of NSDD on the flashover process. From the obtained results, it was found that the leakage current increases with the pollution degree. Nevertheless, non-uniform cases have also been carried out where the effect of pollution distribution on the insulators surface has been the subject of few investigations (e.g., [9]). In these works, the dynamic of flashover discharge was studied using artificial contamination on plane insulator models. Undoubtedly, knowledge of the position and width of the polluted-band on the insulating surface might be one of the most important tasks, leading to better describe the surface state of HV insulators under pollution. Hence, such details might help avoiding the defect on the transmission systems or for having a reasonably accurate assessment of site severity for a technically sound design.

Aiming to describe the surface state of HV insulator model under discontinuous band of desert pollution, the actual paper deals with the extraction of some complementary features based on LC signal records. Experiments have been carried out using an HV insulator plane model having the same leakage path (i.e., 29.2 cm) of 1512L cap-pin insulator widely used in Algerian desert regions. The effect of the applied voltage level, on the discharge activities, has been presented and discussed. Applied voltage of 30 kV has been considered for analysing the LC signal, corresponding to the first stage of the flashover process. The LC signal has been recorded for different positions (HV side, ground side and in the surface midway) and widths of the polluted-band. For each configuration of contamination, LC time-frequency decomposition up to 11 levels has been established using a DWT where the orthogonal Daubechies family has been selected. RP technique and RQA are then applied to the detail D3 since it is highly correlated with the measured LC signal. The indicators RR, DET and ENTR show the effectiveness of RQA applied to D3 as features extraction technique. In fact, RQA indicators are employed to quantify and describe the insulator state under pollution through dynamic the analysis done on the leakage current.

# 2 ARTIFICIAL NON-UNIFORM CONTAMINATION TEST

## 2.1 EXPERIMENTAL SETUP

Figure 1 shows a schematic diagram of the experimental set-up used for analysing the flashover process and the insulator behaviour under various pollution configurations.
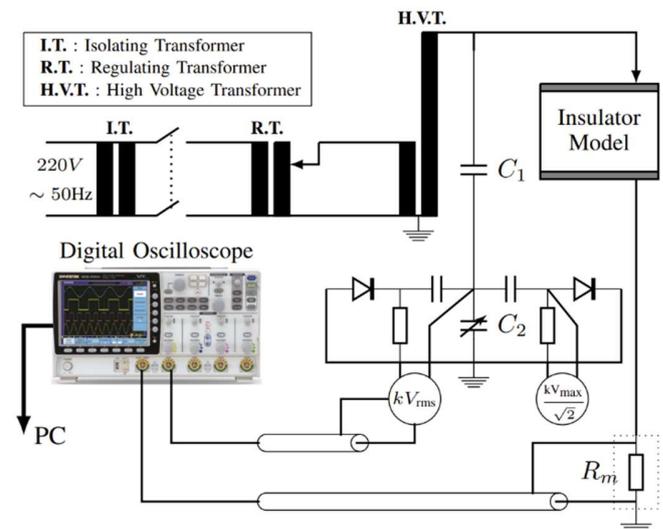


**Figure 1.** Schematic diagram of the experimental set-up

A Haefely transformer (50 kVA, 50 Hz, Icc = 3 A) has been used to generate an AC high voltage up to 300 kV. The primary side voltage can be adjusted using a regulating transformer (50 kVA, 220/500 V, 50 Hz) from the grid voltage of 220 V. Voltage measurements have been achieved using a capacitive voltage divider of 1000:1V ratio (i.e., two capacitances in series : $C_1$ = 400 pF and $C_2$=1000×$C_1$). Leakage current has been recorded from the voltage measurements across a 1-kΩ resistor; inserted between the test cell and the ground. The resistor has been covered by a grounded metal box (of aluminium), forming an electrostatic screen to avoid any external perturbation. INSTEK GDS-3504 Digital Oscilloscope of 500MHz bandwidth, with digitizer of 8 Bits and a maximum sampling rate of 4 GS/s, has been used to visualize the voltage and the current records. The fundamental component ($f_1$ = 50 Hz) is predominant in the voltage waveform, which is characterised by a peak factor of 1.3864 and THD of about 4.95%.

In the actual experiments, the applied voltages satisfy the requirements of IEEE Std 4 [24] and IEC 60060-1 [25], stating that the test voltage distortion should be around 5% and the peak factor should be between 1.344 and 1.485. It is worth noting that the insulator model has been placed horizontally at the height of 175 cm above the ground surface. This can minimize the effect of stray capacitances, which can alter the measurement of the leakage current and the applied voltage.

## 2.1 SAMPLE PREPARATION

A plane glass-model of 50cm×50cm×0.5cm shape has been employed as a test object. This rectangular shape can offer a flexibility and simplicity to control the width of the polluted band. The distance between electrodes of the adopted model is 29.2 cm. It corresponds to the leakage path of 1512L cap-pin insulator largely used in Algerian desert areas. Aluminium paper strips of 50x3x2 cm³ have been used as electrodes where the cutting process has been made carefully so as to avoid creating points. The two electrodes were glued on the glass model surface using diesel fuel to remove void balls, which could lead to the occurrence of premature partial discharges and affect the quality of the measurement.

Several positions of the polluted-band have been considered. For each position, different widths have been selected; ranging from 5 to 25 cm with 5 cm step. Figure 2 presents three positions, in which the polluted-band has been located; (i) near the HV-electrode in Figure 2(a), (ii) near the ground-electrode in Figure 2(b) and (iii) in the midway of the insulator surface as shown in Figure 2(c).
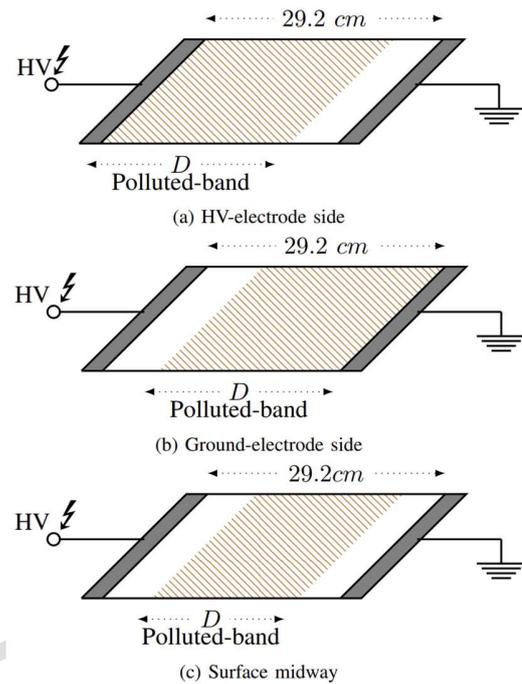


**Figure 2.** Pollution configurations on the HV insulator model

Before each test, the surface of the insulator model is washed with tap water and dried with paper towels, removing any traces that can affect the experiments. In order to avoid any direct electrical path from the end fittings across the insulator surface, the model is cleaned, then after, with isopropyl alcohol and cotton ball soaked in 70% surgical alcohol to ensure maximum cleanliness on the insulating surface. First, the sand has been continuously sprinkled all over a selected band of the model surface. The sand is distributed manually using sieve to avoid any residue parts. In addition, the clean band is recovered by plate of plexiglass. This operation has been accomplished carefully so as to achieve the most uniform polluted layer with the desired width. After that, the polluted band is humidified by spraying distilled water of 2μS/cm-conductivity five times on each side of the model to ensure a good reproducibility of the pollution.

IEC 60815 [23] calls for an estimate of NSDD in the accumulated pollution. Thus, a 0.03g/cm equivalent NSDD has been estimated in the actual investigation, corresponding to 45 g of natural sand. This sand was taken from the desert of El Oued, which is located about 640 km south east of Algeria. The sand samples are taken from a dune at a height of about 20 m. This height is characterized by very fine (between 0.05 and 0.2 mm) and very conductive (1.2 μS/cm) grains of sand since this region is near to Sabkha (i.e., salt soils) that is rich in NaCl.

## 3 RESULTS AND DISCUSSIONS

### 3.1 FLASHOVER PROCESS

The evolution of the flashover process was studied in the literature for uniform and non-uniform configurations of pollution (e.g., [4], [8]). For a polluted-band of relatively small

width (less than 15 cm), it was found that the flashover occurs directly without any preliminary discharge. Otherwise, the flashover process was accomplished by several phases. In order to analyse the flashover process under non-uniform pollution, camera video has been used for the process visualisation. Figure 3 shows an example recorded at four phases corresponding to (i) initiation of arcs on insulator surface, (ii) appearance of several arcs, (iii) critical arc occurrence, and finally (iv) total flashover (shown in Figs. 3(a)—(d), respectively). Such an example has been depicted for a 25cm—width polluted-band situated on the HV-electrode side. Indeed, this width has been selected for a better visualisation of the flashover process.
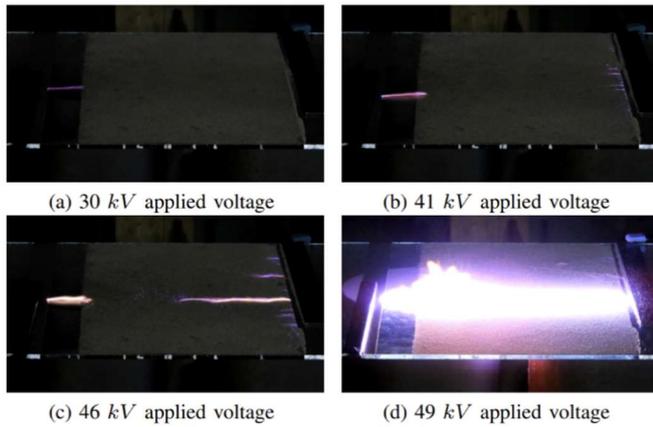


(a) 30 $kV$ applied voltage     (b) 41 $kV$ applied voltage

(c) 46 $kV$ applied voltage     (d) 49 $kV$ applied voltage

**Figure 3.** Flashover process over the applied voltage for 25cm—width polluted-band nearby the HV-electrode side (right side of each photo)

It can be seen from this figure that the initiation of the electric arcs has been established along the clean band on the insulator surface for 30kV-applied voltage. For higher values of the applied voltage, several arcs have appeared on the polluted-band near the HV-electrode side. These arcs have increased in terms of number and length along the polluted band as the applied voltage increased [41 kV in Figure 3(b)]. By further increase of the applied voltage up to 46 kV, leader arcs have been perceived in both sides of the insulator surface, which increased in length while the other arcs progressively disappeared. The leader arcs cause the complete circumvention of the insulating surface non-uniformly polluted at 49kV-applied voltage.

For further comprising the effect of the polluted-band position on the flashover process, the polluted-band has been transmitted to ground-electrode side as well as to the midway of the insulator surface (as shown in Figure 2) by maintaining the previous test conditions. In general, similar processes, as those in Figure 3, have been obtained for different widths of the polluted-band, situated at ground-electrode side as well as at the midway of the insulator surface. Sudden birth of electric arcs has been observed approximately along the clean band. These arcs were developed with further increase in the voltage level, thus, leader arcs propagate until the flashover stage. In other words, the electric field shows a dense concentration at the extremities of the HV insulator model when the applied voltage increases. Then, some arcs initially occur before the surface flashover where practically two leader arcs continue to increase in terms of length, forming the discharge of flashover arc along the surface of the polluted insulator. The applied voltage necessary for each stage of the flashover process depends on the position of the polluted-band.

## 3.2 LEAKAGE CURRENT WAVEFORMS

In this part, applied voltage of 30 kV has been considered for analysing the leakage current since it corresponds to the first stage of flashover process. The LC signal has been recorded for the three aforementioned positions of the polluted-band where several widths have been selected, ranging between 10 and 25 cm with 5 cm step. From left to right, Figure 4 shows examples of the leakage current evolutions, recorded for 10, 15, 20 and 25 cm width of polluted-band. For each width, the three aforementioned positions have been considered. Figure 4(a) [respectively, Figure 4(b)] shows the obtained results for pollution near the HV-electrode (respectively ground-electrode) side. For polluted-band situated on the midway of the insulating surface, the measured results have been illustrated in Figure 4(c).

It is shown that the position and width of the polluted-band have a significant influence on the LC waveforms as well as on the behaviour of the insulator model under non-uniform pollution. For all positions of polluted-band in Figure 5, the insulator behaviour is predominantly capacitive for small widths (e.g., 10 cm) of the polluted-band, becoming gradually resistive at larger widths (e.g., 20 cm). Capacitive effects are larger in the case of pollution in the midway of the insulator surface compared to the other positions since the LC signals are in advance on the applied voltage waveform. With the increase (respectively, decrease) of the clean (respectively, polluted) band between electrodes, the amount of charges induced on the total area of each conductor increases, which decreases the LC signals. This implies that the LC waveforms are distorted because of the capacitive behaviour of the clean band that amplifies the magnitude of the LC odd harmonics as stated in [26]. Table 1 illustrates the phase angle computed between the applied voltage signal and the measured LC.

**Table 1.** Phase angle (in degree) between applied voltage and LC

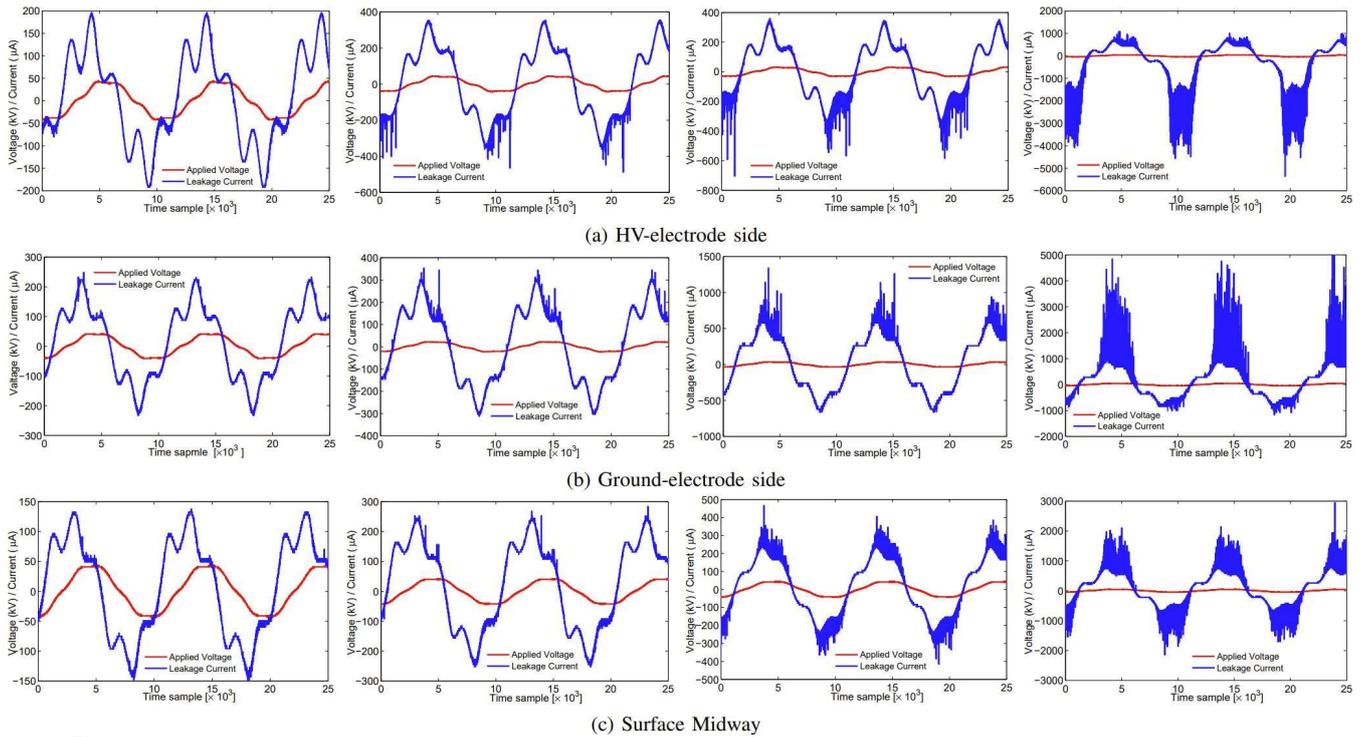| Position | Selected width | | | |
|---|---|---|---|---|
| | 5 cm | 15cm | 20 cm | 25cm |
| HV-side | 61.86 | 37.50 | 34.37 | 13.17 |
| GR-side | 50.11 | 46.25 | 37.52 | 20.89 |
| Midway | 64.87 | 60.02 | 27.74 | 20.85 |

**Figure 4.** LC waveforms recorded for different pollution-band positions and widths (from left to right: D = 10, 15, 20 and 25cm) under 30kV voltage

Such findings are in agreement with those reported in other published works (e.g., [13], [15]), in which the authors concluded that the phase angle is a suitable quantity to study the insulator behaviour. Moreover, Figure 4 clearly shows a large number of spikes in positive and/or negative half-cycles of LC waveforms. These spikes, increased with the polluted-band width, can indicate the appearance of high-frequency components on the recorded current waveforms. For polluted-band positioned at the HV-electrode (respectively ground-electrode) side in Figure 4(a) (respectively Figure 4(b)), the spikes appear on the negative (respectively positive) half-cycle of the LC signal. On the other hand, the high-frequency pulses have been observed on both half-cycles in Figure 4(c) for pollution located in the midway of the insulator surface. Table 2 gives the RMS values of LC for different positions and widths of the polluted-band.

**Table 2.** RMS of LC in µA

| Position | Selected width | | | |
|---|---|---|---|---|
| | 5 cm | 15cm | 20 cm | 25cm |
| HV-side | 91.39 | 193.03 | 250.29 | 1132.60 |
| GR-side | 80.34 | 130.51 | 377.00 | 848.80 |
| Midway | 61.87 | 72.70 | 308.97 | 559.00 |

From these results, the LC magnitude gradually increases with the pollution width. The amount of augmentation for the polluted-band on the ground-electrode side is much higher than that at the HV-electrode side. For a pollution located at the HV-electrode side, for instance, the high-frequency peaks increases by up to 29.66% when the pollution width is increased from 15 to 20 cm, whereas for a pollution near the ground-electrode side, the increase in high-frequency peaks is 188.87%.

The leakage current, driven by the source voltage and collected at the grounded end of the insulator, provides much useful information out of many parameters describing the state of a contaminated glass insulator model. Such an ascertainment proves the capability of LC signals for indicating the polluted-band location on the insulator surface. This is to say that the highest current peaks recorded in the leakage current measurements announce the presence of arcs on the insulating surface, and the presence of the pollution as well. Indeed, pollution nearby HV-electrode side, ground-electrode side and in the midway have been concluded, respectively, from negative, positive and negative-positive signs of high-frequency pulses in the LC signal. Moreover, the characteristics of LC waveforms might be investigated by applying signal processing techniques to quantitatively clarify their influence on the insulator behaviour, describing the state of a contaminated insulator.

### 3.3 HIGH-FREQUENCY DECOMPOSITION

In this part, investigations have been conducted with regard to the frequency characteristics of LC waveforms. Significant information in LC signal is concentrated in the 0—250 kHz band. Applying the Shannon's theorem yields a minimum sampling frequency of 500 kHz. Consequently, sampling frequency fs = 500 MHz has been chosen in this investigation corresponding to that of the digital oscilloscope. Hence, Ns = 25000 samples have been acquired with a resolution of 0.05 Hz according to [27].

DWT has been established to detect frequency components of the measured LC under non-uniform pollution. In fact, it allows to break down the signal of the LC into several frequency components, condensing the information of a large set of correlated variables into a few variables while not throwing overboard the variability present in the data set. DWT is commonly used in signal processing to detect and filter white Gaussian noise, enhancing signal-to-noise-ratio. For this reason, the LC has been gone through a bandpass filter for the

targeted purpose. Several types of mother wavelets can be used such as biorthogonal, coiflet, simlet and so on. Some authors showed that the whole of these mother wavelets (with different properties) gave practically similar results. Because of its well-known properties, the orthogonal Daubechies family has been chosen in the present investigation. Using "db4" mother wavelet, the LC of polluted configuration has been decomposed in up to 11—levels.

In previous works (e.g., [4],[9]), the STD was investigated to find the most significant details for the purpose of monitoring the insulator surface. STD representation of details D10 and D11 showed a good correlation with the NSDD increase in uniform pollution configuration. For a given NSDD, otherwise, D11 and D1 to D6 were in good correlation with the polluted layer width increase in non-uniform pollution configuration. In addition, details D1 to D6 are effective to provide information about the electric discharges and they might be used as good indicators to describe the electric discharges activity on the insulator surface. However, it was found that the third harmonic magnitude is of importance compared to other odd harmonics in non-uniform pollution configuration. Such findings have been interpreted (in accordance with other researches [1], [10]) by the presence of arcs behind the considerable increase of the LC magnitude. In other words, the detail D3 is highly correlated with the recorded signal in the time domain. In this light, the evolution in the observed frequency bands of the signal component associated to the insulator model defect (shown in Figure 5) has been analysed using the D3 details.

While analysing the effect of the insulator defect in the bands of the frequencies of interest in Figure 5, one can see that the energy stored in the studied signal depends on the width of the polluted-band. For all studied positions, this effect is interpreted by the increase in terms of amplitude of the signals in D3 bands. Indeed, the effect of the extraction of the details

D3 of the LC also leads to a differentiation in the energies stored in the levels between the various positions, especially in the case of pollution in the midway of the insulating surface. According to the obtained results, however, one can note that the previous effect in terms of stored energy is similar for polluted-band situated on both sides of the insulator model. Summarizing, the use of the wavelet technique enables us to locate and to describe the pollution layers on the insulator surface from the leakage current signals. For better information extraction in a quantitative term, the next section of this investigation elaborates the recurrence plot technique followed by recurrence quantification analysis.

# 4  RP AND RQA APPLIED TO THE LC

## 4.1 RP STRUCTURES

The leakage current (LC) is given by time-series visualization of M samples as follows:

$$LC = [x(1), x(2), . x(2), . . . . , x(M)] \qquad (1)$$

In this technique, LC has been represented by space phases $X$ of N dimension and $m$ embedding with time delay of $\tau$ as follows [28]:

$$X_i = \sum_{k=1}^{m} x[i + (k-1)\tau] . e_k \qquad (2)$$

in which, $e_k$ is the axis unit vectors corresponding to each dimension of the phase-space. The embedding $m$ and the time delay $\tau$ of the space phases have been chosen equal to 5 and 20, respectively, according to [29]. The tenser (R) of RP map has been computed by [28]:

$$R_{i,j} = H\left(\varepsilon - \left\| \vec{X}(i) - \vec{X}(j) \right\|\right) \qquad (3)$$



(a) HV-electrode side
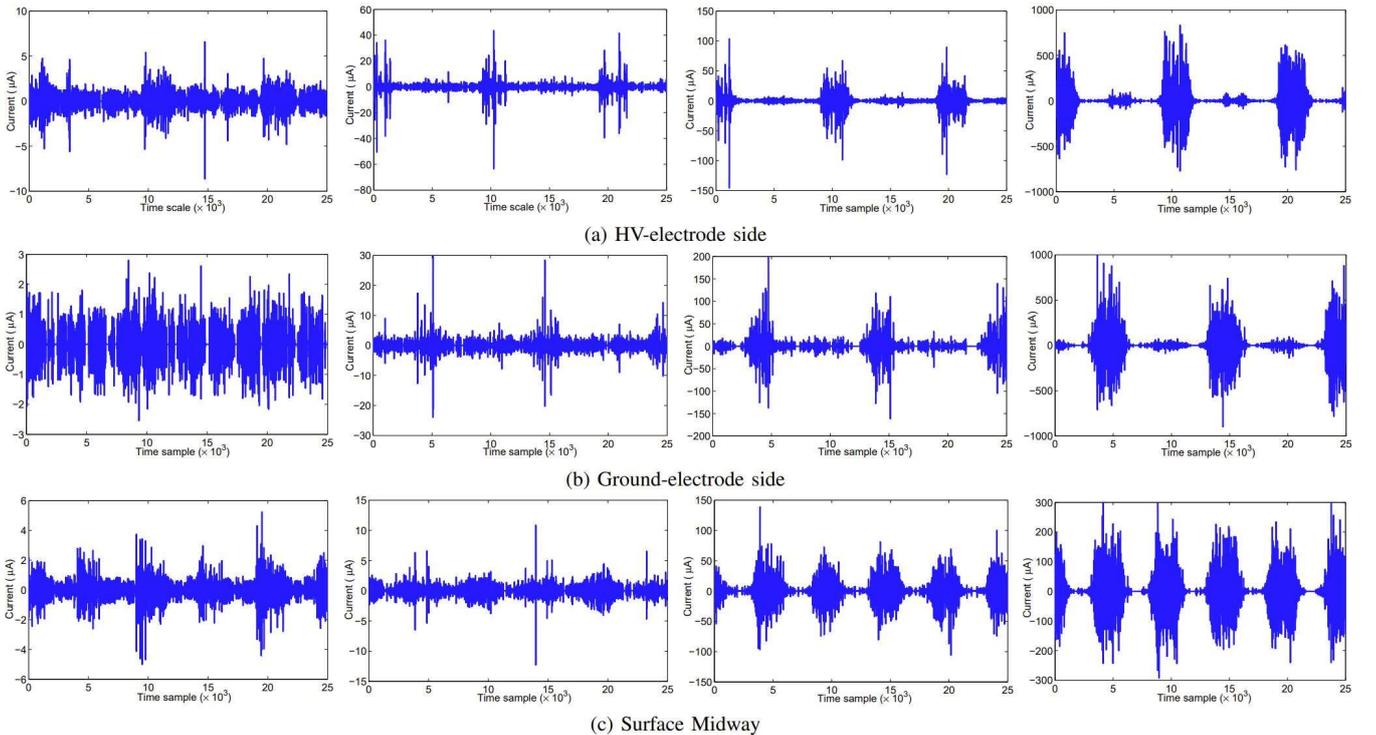
(b) Ground-electrode side

(c) Surface Midway

**Figure 5.** LC high-frequency components for different pollution-band positions and widths (from left to right: $D = 10, 15, 20$ and $25cm$)

where ‖·‖denoted the Euclidean norm (other norms might be adopted), $X$ is the studied space phase and $H(\cdot)$ the Heaviside function. It is worth noting that high values of $\varepsilon$ increment the density of recurrence points in the recurrence plot, while smaller values lead to inadequate population of the recurrence points. The threshold $\varepsilon$ is considered constant, equal to 0.25×STD ; STD is the signal standard deviation. Table 3 illustrates the STD values of LC for different positions and widths of the polluted-band.

**Table 3.** STD values obtained from LC

| Position | Selected width | | | |
|---|---|---|---|---|
| | 5 cm | 15cm | 20 cm | 25cm |
| HV-side | 61.86 | 73.5 | 39.84 | 13.17 |
| GR-side | 50.11 | 46.25 | 37.52 | 20.89 |
| Midway | 61.18 | 71.27 | 306.21 | 10.55 |

Expression (3) means that if the distance between $X_i$ and $X_j$ is less than the value of the threshold $\varepsilon$, the tenser $R_{ij} = 1$ associated by a dot (colored point) at the corresponding location $(i, j)$ in the RP plot, otherwise $R_{ij} = 0$ with a blank point on the RP map. Figure 6 illustrates an example of the RP maps obtained from D3 (shown in Figure 5) of the LC high-frequency extract. The results have been obtained from different widths of the polluted-band (D = 10, 15, 20 and 25 cm) located on the HV-electrode side.
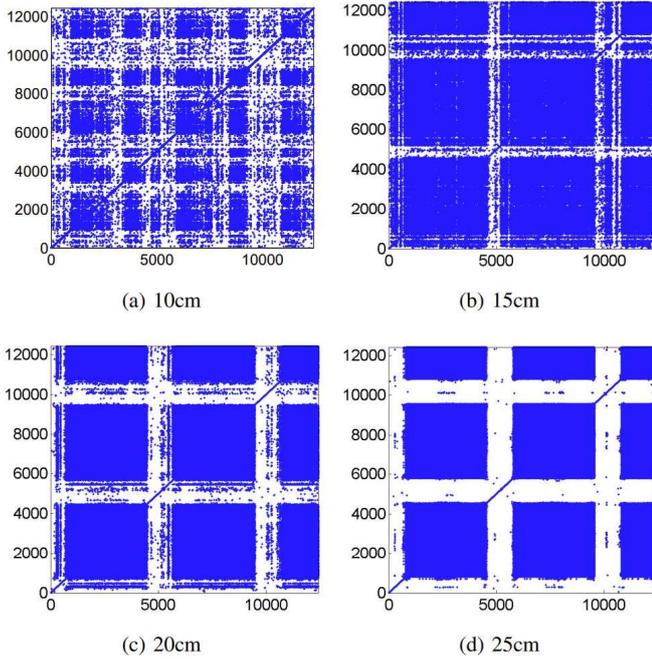


(a) 10cm

(b) 15cm

(c) 20cm

(d) 25cm

**Figure 6.** RP maps of D3 components for polluted-band on HV-electrode side for different widths under 30 kV applied voltage

It is clear that RP structures are composed of dense points grouped into rectangles, isolated points, and blank bands. As can be seen from these figures, the concentration of recurring points, the location and the number of blank bands on the RP maps mainly depend on the width of the polluted-band. For small widths of the polluted-band, RP maps show a low density of the recurrent points accompanied by a large number of isolated points. The concentration of these points increases with

the width of the polluted-band, and the blank bands on the RP maps increases as well. It should be noted that the morphology of RP structure has been varying with regards to the considered positions of the polluted-band. In general, the obtained results show the possibility to extract information regarding the insulator state from RP technique applied to high-frequency components of the LC. However, analyzing the graphical topology of RP maps might be quite difficult. For this purpose, RQA has been used in the next part to quantitatively describe the graphical and morphological structures of the RP maps as shown in Figure 6.

## 4.2 RQ ANALYSIS

In contrast to the heuristic approach of the RQ analysis, some dynamical invariants as correlation dimension, entropy or mutual information (independent on the embedding) have been derived from RP maps. The base for these dynamical invariants are the recurrence rate and distribution of the lengths of the diagonal lines, as given below [28]:

a. RR values show the density of the recurrence points on the RP maps. It is given by:

$$RR = \frac{1}{N^2} \sum_{i=1}^{N} \sum_{j=1}^{N} R_{i,j} \qquad (4)$$

which expresses the measure of ability for the system to return about previous states.

b. DET is the measure of predictability of the examined time series (i.e., LC signals), and it gives the ratio of the recurrence points formed in diagonals to all recurrence points. It is expressed by:

$$DET = \frac{1}{N^2 RR} \sum_{\ell = \ell_{min}}^{N} \ell P(\ell) \qquad (5)$$

in which, $\ell$ is the length of the diagonal lines, $P(\ell)$ is the number of diagonal lines of exactly length $\ell$ in the RP map. The quantity $\ell_{min}$ is the threshold, which excludes the diagonal lines formed by the tangential motion of a phase space trajectory.

c. ENTR refers to Shannon entropy of the probability to find a diagonal line having exactly a length equal to $\ell$ in the RP maps. This quantity is given as follows:

$$ENTR = \frac{1}{N} \sum_{\ell=1}^{N} P(\ell) \ln\left(\frac{P(\ell)}{N}\right) \qquad (6)$$

which quantifies the frequency distribution of the diagonal line length.

The aforementioned parameters have been computed and their average values have been illustrated in Figure 7 for different widths and positions of the polluted-band.

Very low values of RR (less than 0.1) have been noticed for polluted-band widths of 10 and 15 cm. RR increases towards a maximum value of about 0.4 when the pollution width increases to 20 and 25 cm. These widths have been characterized by high electric discharges activity (Figure 3). In comparison between the positions of the polluted-band, RR
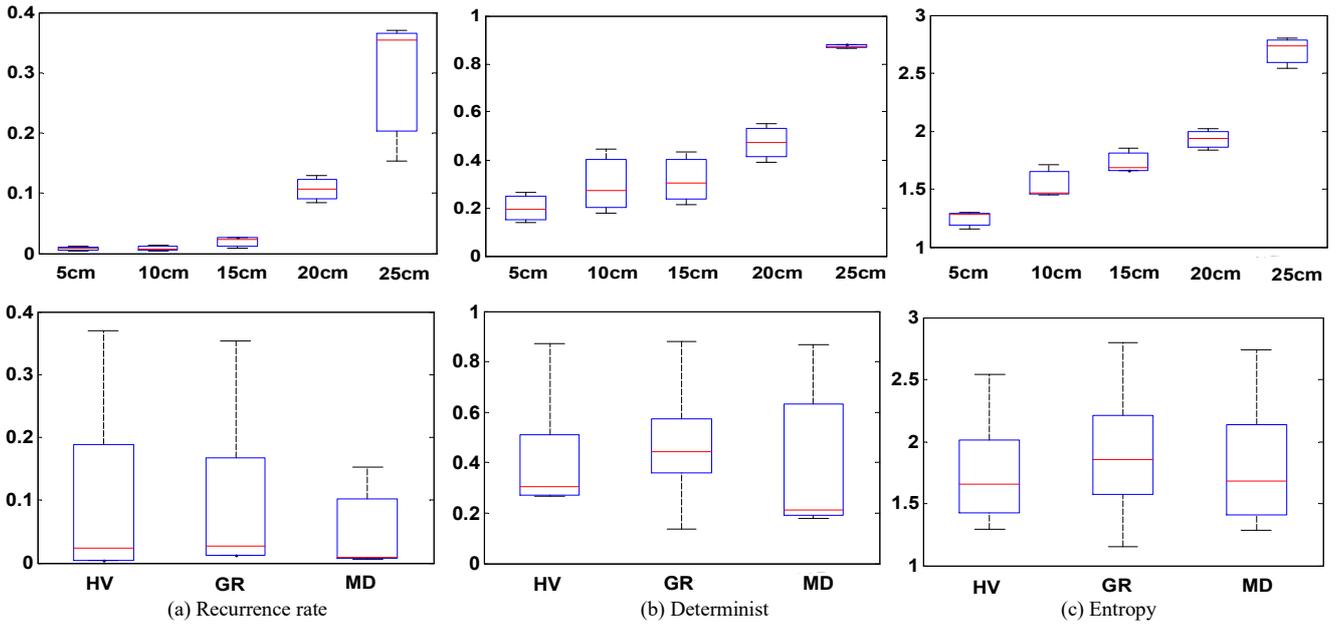
**Figure 8.** RQ indicators of RP map applied on the high-frequency components for several widths and positions of the polluted-band at 30kV voltage

values are more important for pollution situated at the GR-electrode side than those obtained for polluted-band located at the HV-electrode side. Both positions are characterized by higher values of RR compared to the third case of polluted-band position. The indicator DET differentiates isolated recurrent points from those connected with each other in the diagonal direction. A smaller value of DET denotes that the investigated system has a less deterministic ingredient. The increasing of the DET indicates that the signals become more deterministic.

For each polluted-band position, the low values of the DET (around 0.25), corresponding to 10 and 15 cm of the pollution widths, indicate a stochastic dynamic behavior of the high frequency components signal, and the important DET values (between 0.5 and 0.8), related to 20 and 25 cm of pollution widths, indicate that the signals are more deterministic. On the other hand, ENTR shows approximately a linear variation with regard to the width of the polluted-band, starting from 1.2 to 2.8 for widths ranging between 10 to 25 cm. The increase of the ENTR values indicates an increase of the periodicity of the high frequency components in the investigated signal. Indeed, large values of ENTR indicate the changing complexity of the leakage current waveform, which becomes periodical for the large widths of polluted-band.

Overall, it was found that RQA indicators increase with the polluted-band widths whatever the position of this polluted band. Therefore, RQA indicators variation quantifies and describes the insulator model state under pollution through dynamic the analysis done on the leakage current. In other words, the deterioration of the insulator model performance is highlighted by the increase within the RQA indicators, which are related to the width and position of the polluted-band. In general, higher values of these indicators announce the shifting of LC signal from periodical dynamic to non-stationary one, indicating the presence of discharge activities and, hence, the possible occurrence of a flashover. Moreover, RQA indicators

are related to each position of the three polluted-band configurations. This ascertainment demonstrates the capability of the RQA indicators to differentiate between the three positions of the polluted-band. Finally, these three indicators as well as other conventional parameters such as the mean value of LC, the maximum value of LC, the phase angle, the STD and the THD seem to be effective features those might be used to monitor the surface state of high voltage insulators. In fact, these features might be helpful for the diagnosis of HV insulators under pollution conditions. To achieve better monitoring and classification results as well as to increase the credibility of the results, more experiments are required using different insulators, different types of sand, various applied voltage levels and so on.

## 5 CONCLUSIONS

This paper addressed a complementary investigation for the extraction of features characterizing a non-uniformly polluted HV insulator model, giving information on the width and position of the polluted-band. Experimental tests on non-uniformly polluted insulators were conducted where a plane model with a leakage path of 29.2 cm was used.

Examples of flashover processes were presented and the LC signal was recorded for different positions and widths of the polluted-band. It was found that the initiation of the electric arcs was established along the clean band on the insulating surface. As the applied voltage increased, these arcs were increased in terms of number and length along the surface of the insulator model. By further increase of the applied voltage, leader arcs were persisted in both sides of the insulator surface, which increased in length while the other arcs progressively disappeared. The leader arcs cause the complete circumvention of the insulating surface non-uniformly polluted. Indeed, the

leakage current waveform represents an important source of information to describe the surface state of the insulator model.

For each configuration, a discrete wavelet technique was elaborated for LC time-frequency decomposition. An increase in terms of amplitude was found in the detail D3 with regards to the width of the polluted-band. For better information extraction in a quantitative term, recurrence plot technique and recurrence quantification analysis were elaborated, and the high-frequency components of LC (detail D3) was used for the extraction purpose. From the obtained results, RQA main indicators (i.e., RR, DET and ENTR) showed a strong correlation with the flashover process. For instance, very low values of RR (less than 0.1) were obtained for polluted-band of widths less than 15 cm. The RR increases with the width towards a maximum value of about 0.4 found at 25 cm width. Moreover, the indicator DET differentiated isolated recurrent points from those connected with each other in the diagonal direction. ENTR shows approximately a linear variation with regard to the width of the polluted-band, starting from 1.2 to 2.8 for widths ranging between 10 to 25 cm. The variation range of these indicators help identifying the position of the polluted band.

Finally, these three indicators as well as other conventional parameters such as the mean value of LC, the maximum value of LC, the phase angle, the STD and the THD represent effective features for monitoring the surface state of high voltage insulators. To achieve better monitoring and classification results as well as to increase the credibility of the results, more experiments are required using different real insulators, different types of sand, various applied voltage levels.

## ACKNOWLEDGMENT

## REFERENCES

[1] G.O.E. Gouda and A. El-Dein, "Experimental techniques to simulate naturally polluted high voltage transmission line insulators," IEEE Trans. Dielectr. Electr. Insul., vol. 21, no. 5, pp. 2199–2205, Oct. 2014.

[2] Y. Mizuno, H. Kusada and K. Naito, "Effect of Climatic Conditions on Contamination Flashover Voltage of Insulators," IEEE Trans. Dielectr. Electr. Insul., vol. 4, no. 3, pp. 286–289, Jun. 1997.

[3] A. Mekhaldi, D. Namane, S. Bouazabia and A. Beroual, "Flashover of Discontinuous Pollution Layer on HV Insulators," IEEE Trans. Dielectr. Electr. Insul., vol. 6, no. 6, pp. 900–906, Dec. 1999.

[4] D. Maadjoudj, A. Mekhaldi and M. Teguar, "Flashover Process and Leakage Current Characteristics of Insulator Model under Desert Pollution", IEEE Trans. Dielectr. Electr. Insul, vol. 25, no. 6, pp. 2296 2304, Dec. 2018.

[5] D. Maadjoudj, A. Mekhaldi and M. Teguar, "Frequency Analysis and Recurrent Plot of the Leakage Current to Monitoring the Insulator Surface State", in Prooc. The IEEE 2nd Int. Conf. Dielect. (ICD), Budapest, Hungary, Jul. 1-5, 2018.

[6] Z. Zhang, Y. Dongdong and X. Jiang, "AC Flashover Performance of various types of Insulators under Fan-shaped Non-uniform Pollution," IEEE Trans. Dielectr. Electr. Insul., vol. 23, no. 3, pp. 1760–1768, Jun. 2016.

[7] W. Sima, Q. Yang, G. Ma, C. Jiang, L. Wu and H. Chen, "Experiments and Analysis of Sand Dust Flashover of the Flat Plate Model," IEEE Trans. Dielectr. Electr. Insul., vol. 17, no. 2, pp. 572–581, Apr. 2010.

[8] M.A. Slama, A. Maurizio, A. Haddad, R.T. Waters, O. Cwikowski, I. Iddrissu, J. Knapper, and O. Scopes, "Monitoring of Dry Bands and Discharge Activities at the Surface of Textured Insulators with AC Clean Fog Test Conditions" Energies 14, no. 10, pp. 2914, 2021.

[9] D. Maadjoudj, A. Mekhaldi and M. Teguar, "Wavelet transform of the leakage current to monitoring the insulator surface under non-uniform desert pollution", in Prooc. 3rd CISTEM-2018, Algiers, Algeria, Oct. 29-31, 2018.

[10] T. Suda, "Frequency Characteristics of Leakage Current Waveform of an Artificially Polluted Suspension Insulator," IEEE Trans. Dielectr. Electr. Insul., vol. 8, no. 4, pp. 705–709, Aug. 2001.

[11] J. Li, W. Sima and C. Sun, "Use of Leakage Currents of Insulators to Determine the Stage Characteristics of the Flashover Process and Contamination Level Prediction," IEEE Trans. Dielectr. Electr. Insul., vol. 17, no. 2, pp. 490–501, Apr. 2010.

[12] M. Fernando and S.M. Gubanski, "Leakage Current Patterns on Contaminated Polymeric Surfaces," IEEE Trans. Dielectr. Electr. Insul., vol.6, no. 5, pp. 688–694, 1999.

[13] X. Jiang, Y. Shi, C. Sun and Z. Zhang, "Evaluating the Safety Condition of Porcelain Insulators by the Time and Frequency Characteristics of LC Based on Artificial Pollution Tests," IEEE Trans. Dielectr. Electr. Insul., vol. 17, no. 2, pp. 481–489, Apr. 2010.

[14] B. Moula, A. Mekhaldi, M. Teguar and A. Haddad, "Characterization of Discharges on non-Uniformly Polluted Glass Surfaces Using a Wavelet Transform Approach," IEEE Trans. Dielectr. Electr. Insul., vol. 20, no. 4, pp. 1457–1466, Aug. 2013.

[15] A. Chaou, A. Mekhaldi and M. Teguar, "Recurrence Quantification Analysis as a Novel LC Feature Extraction Technique for the Classification of Pollution Severity on HV Insulator Model," IEEE Trans. Dielectr. Electr. Insul., vol. 22, no. 6, pp. 3376–3384, Dec. 2015.

[16] Y. Liu and B.X. Du, "Recurrent Plot Analysis of Leakage Current in Dynamic Drop Test for Hydrophobicity Evaluation of Silicone Rubber Insulator," IEEE Trans. Power Del., vol. 28, no. 4, pp. 1996–2003, Oct. 2013.

[17] N. Bashir and H. Ahmad, "Odd Harmonics and Third to Fifth Harmonic Ratios of Leakage Currents as Diagnostic Tools to Study the Ageing of Glass Insulators," IEEE Trans. Dielectr. Electr. Insul., vol. 17, no. 3, pp. 819–832, Jun. 2010

[18] M. Faramarzi and M. Mirzaire, "Diagnosis of porcelain and glass insulators conditions using phase angle index based on experimental tests," IEEE Trans. Dielectr. Electr. Insul., vol. 23, no. 3, pp. 1460– 1466, Jun. 2016.

[19] N. Megriche and A. Beroual, "Time-frequency analyses of leakage current waveform and non-uniform polluted conditions," IET Sci. Meas. Tech., vol. 9, no. 8, pp. 945–954, Nov. 2015.

[20] H. Kordkheili, H. Abravesh and M. Tabasi "Determining the Probability of Flashover Occurrence in Composite Insulators by Using Leakage Current Harmonic Components," IEEE Trans. Dielectr. Electr. Insul., vol. 17, no. 2, pp. 502–512, Apr. 2010.

[21] D. Maadjoudj, A. Mekhaldi and M. Teguar, "Recurrent Plot and Quantification of Leakage Current for Monitoring the Insulator Surface State under Nonuniform Desertic Pollution ", in Prooc. Int. Conf. Elec. Engin. (ICEE-B), Boumerdes, Algeria, Oct. 29-31, 2017.

[22] Y. Liu, M. Farzaneh and B.X. Du, "Nonlinear Characteristics of Leakage Current for Flashover Monitoring of Ice-covered Suspension Insulators," IEEE Trans. Dielectr. Electr. Insul., vol. 23, no. 3, pp. 1242–1250, Jun. 2016

[23] Guide for the Selection of Insulators in Respect of Polluted Conditions, IEC 60815, Ed. 1.0, 2008.

[24] IEEE Standard for High-Voltage Testing Techniques. IEEE Standard 4-2013, 2013 (Revision of IEEE Std 4-1995).

[25] High-voltage test techniques, General Definitions., IEC 60060-1, 2010.

[26] M. A. Douar, A. Mekhaldi, and M. C. Bouzidi, "Flashover process and frequency analysis of the leakage current on insulator model under non-uniform pollution conditions," IEEE Trans. Dielectr. Electr. Insul., vol. 17, Nn. 4, pp. 1284-1297, 2010.

[27] Z. Cvetkovic and M. Vetterli, "Discrete-time wavelet extreme representation: Design and consistent reconstruction," IEEE Trans. Signal Process., vol. 43, no. 3, pp. 681–693, Mar. 1995.

[28] N. Marwan, M. Riley, A. Giuliani and C.L. Webber, Translational Recurrences: From Mathematical Theory to Real-World Applications., (Springer International Publishing, Switzerland, 2014).

[29] A. Facchini, C. Mocenni, N. Marwan, A. Vicino and E. Tiezzi, "Nonlinear time series analysis of dissolved oxygen in the Orbetello Lagoon," Ecological Modeling, vol. 3–4, pp. 339–348,